

Supporting information

Impact of dye end groups on acceptor-donor-acceptor type molecules for solution-processed photovoltaic cells

Guangrui He,¹ Zhi Li,¹ Xiangjian Wan,¹ Yongsheng Liu,¹ Jiaoyan Zhou,¹ Guankui Long,¹ Mingtao Zhang,² Yongsheng Chen^{1,*}

Section A tables and figures

Table S1. d-Spacing values of the conjugated molecules.

Compounds	d ₁₀₀ (Å)	d ₂₀₀ (Å)	d ₃₀₀ (Å)
D2R(8+2)7T	-	-	-
DTDMP7T	19.0	-	-
DERHD7T	19.3	9.6	6.4
DCAO7T	21.0	10.5	7.0

Table S2. Summary of device performance for various BHJ devices based on D2R(8+2)7T and DTDMP7T in the work.

Active Layer	Ratio (w/w)	V _{oc} /V	J _{sc} / mA cm ⁻²	FF(%)	PCE(%)
D2R(8+2)7T: PC ₆₁ BM ^a	1:0.3	0.92	4.33	34	1.37
D2R(8+2)7T: PC ₆₁ BM ^a	1:0.5	0.92	6.77	39	2.46
D2R(8+2)7T: PC ₆₁ BM ^b	1:0.5	0.90	6.16	37	2.06
D2R(8+2)7T: PC ₆₁ BM ^a	1:0.7	0.92	5.88	36	1.96
DTDMP7T: PC ₆₁ BM ^a	1:0.5	0.80	6.62	58	3.05
DTDMP7T: PC ₆₁ BM ^a	1:0.8	0.90	7.54	60	4.05
DTDMP7T: PC ₆₁ BM ^b	1:0.8	0.88	6.51	37	2.10
DTDMP7T: PC ₆₁ BM ^a	1:1	0.90	6.64	52	3.12

a: device with Ca/Al as cathode; **b:** device with LiF/Al as cathode.

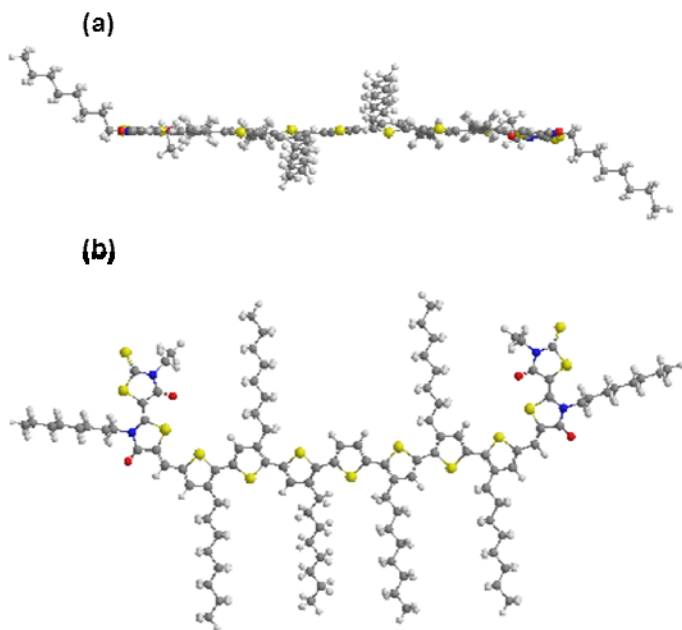


Figure. S1 (a) top view (b) side view of molecular structure of D2R(8+2)7T. The molecular geometry was optimized by Gaussian09 program, using the Density Functional Theory (DFT) with the PBE1PBE/6-31G(d) basis set and frequency analysis was followed to assure that the optimized structures was stable states^[1].

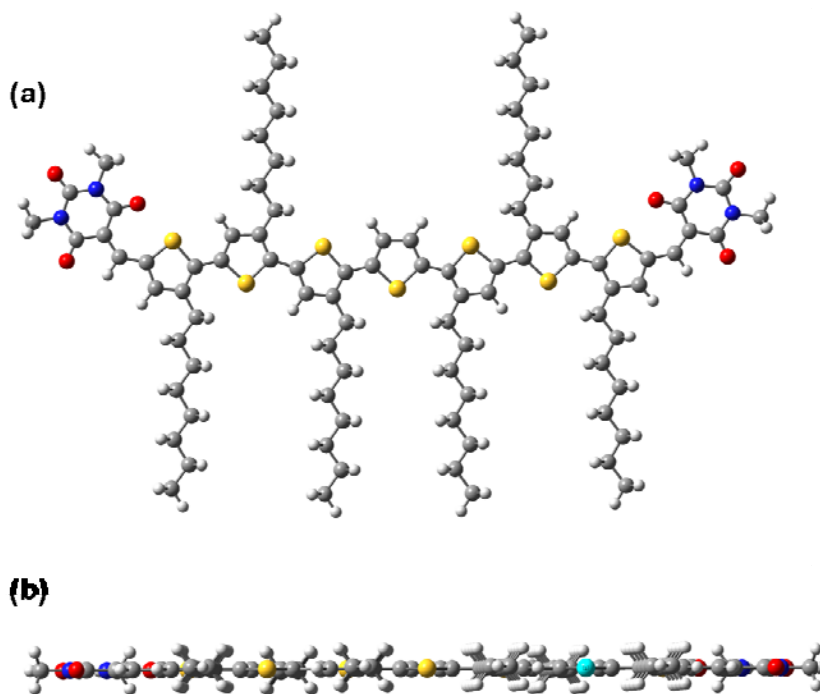


Figure. S2 (a) top view and (b) side view of molecular structure of DTDMP7T^[1].

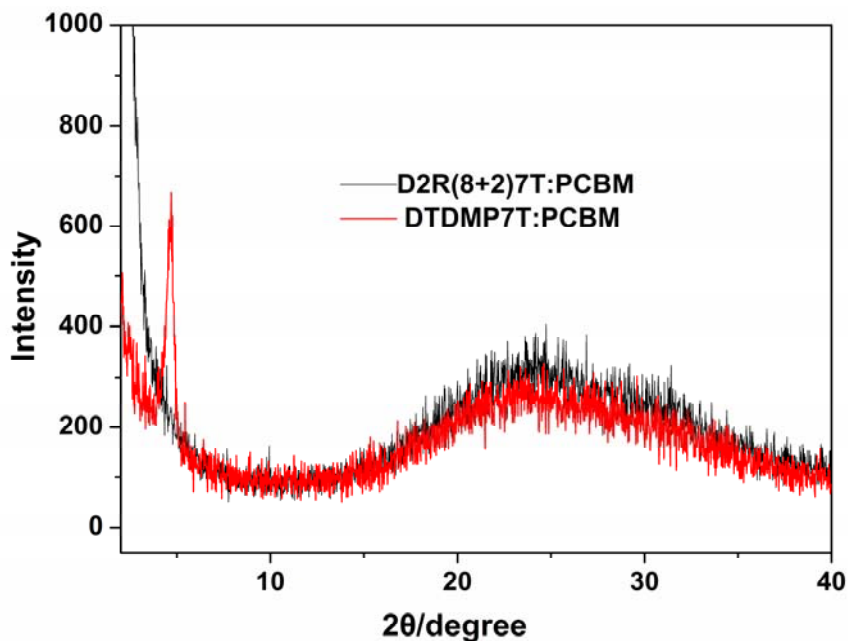


Figure S3. XRD (X-Ray diffraction) patterns of D2R(8+2)7T/PC₆₁BM (w:w=1:0.5) and DTDMP7T/PC₆₁BM (w:w=1:0.8) film spin-coated from CHCl₃ onto glass substrate, the broad peak from 18° to 35° attributed to the signal of glass.

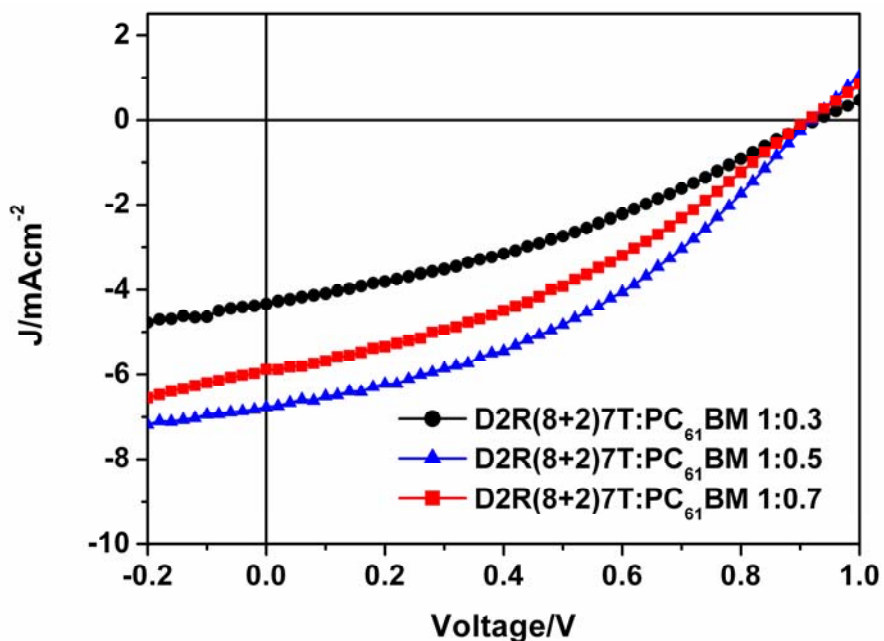


Figure S4. Characteristic *J-V* curves of BHJ solar cells based D2R(8+2)7T/PC₆₁BM with blend ratios (w:w) of 1:0.3, 1:0.5 and 1:0.7 with Ca/Al as the cathode under illumination of AM 1.5 G, 100 mW cm⁻².

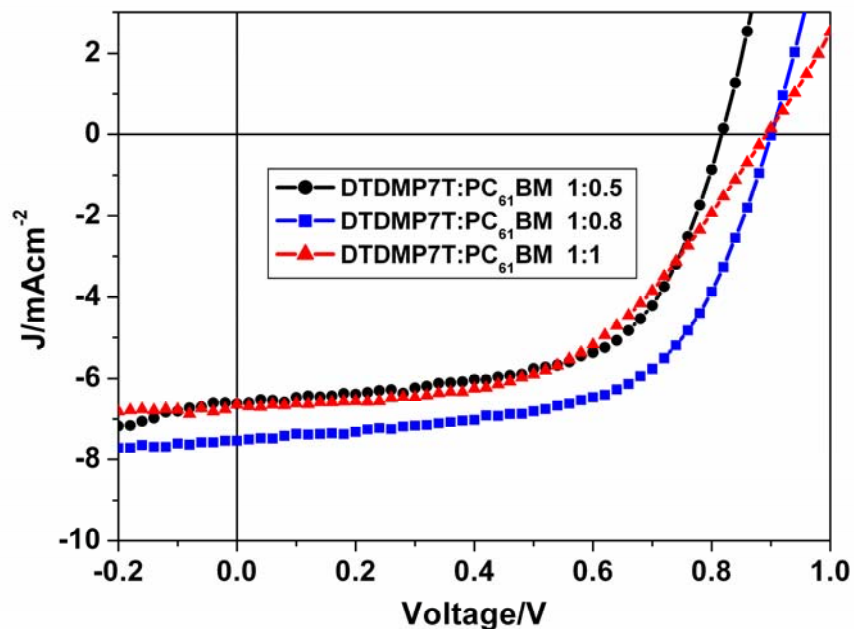


Figure S5. Characteristic J - V curves of BHJ solar cells based DTDMP7T/PC₆₁BM with blend ratios (w:w) of 1:0.5, 1:0.8 and 1:1 with Ca/Al as the cathode under illumination of AM 1.5 G, 100 mW cm⁻².

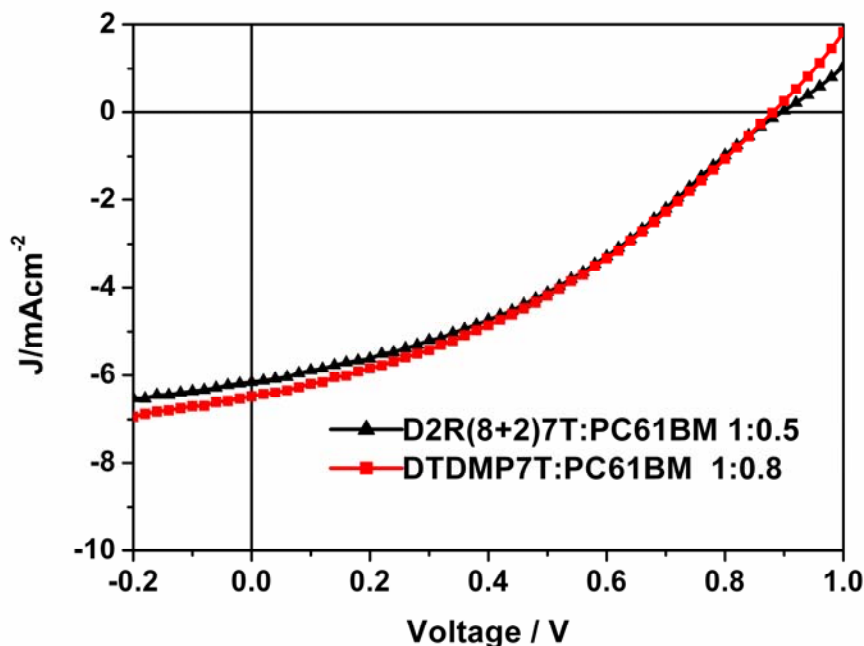


Figure S6. Characteristic J - V curves of BHJ solar cells based D2R(8+2)7T/PC₆₁BM and DTDMP7T/PC₆₁BM with optimized blend ratios (w:w) of 1:0.5 and 1:0.8 with LiF/Al as the cathode under illumination of AM 1.5 G, 100 mW cm⁻².

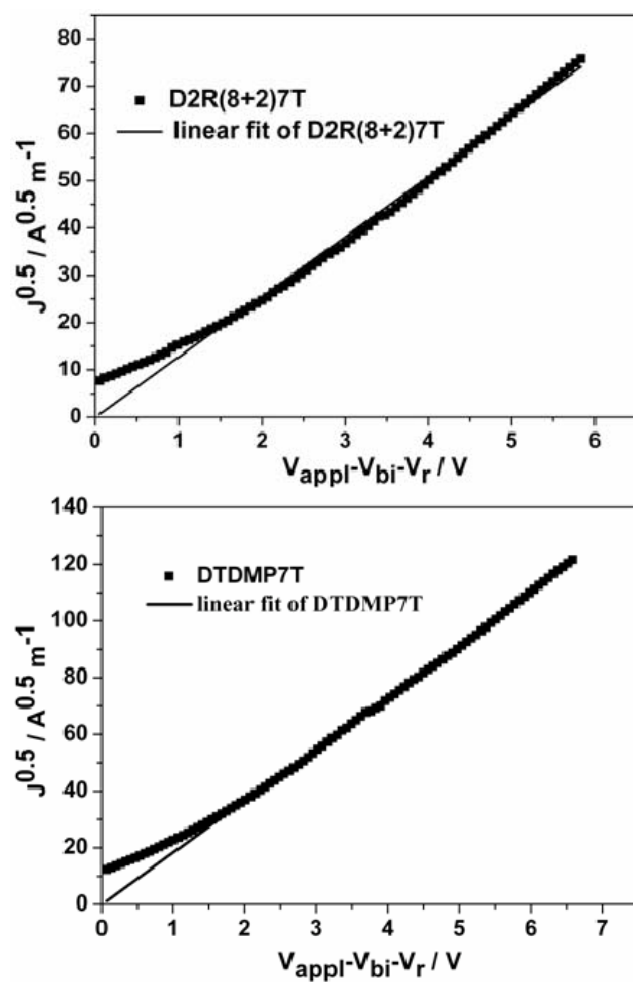


Figure S7. $J^{0.5}$ vs V plots for the pure D2R(8+2)7T and DTDMP7T films at room temperature.

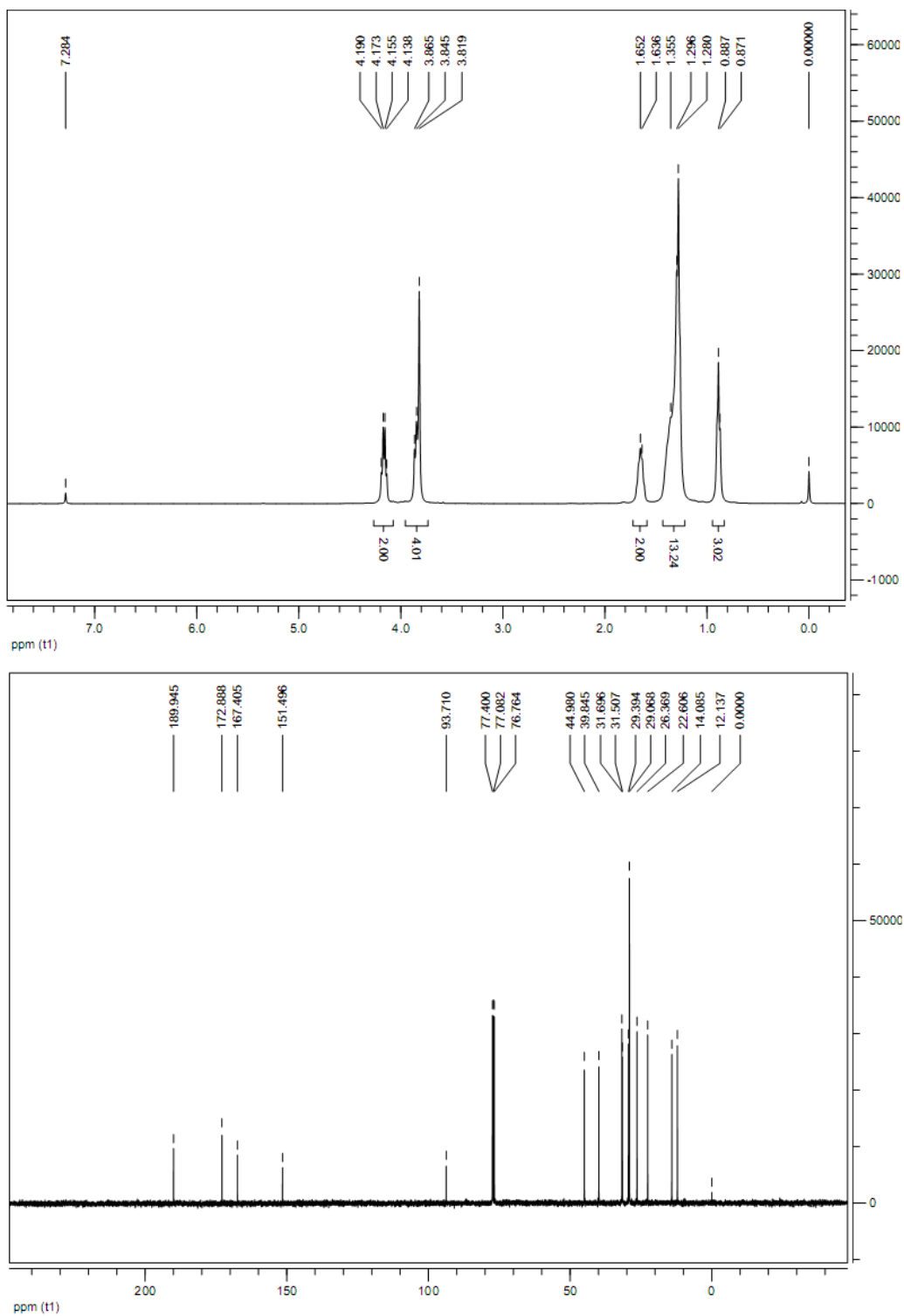


Figure S8. ¹H NMR (top) and ¹³C NMR (below) spectrums of D2R(8+2).

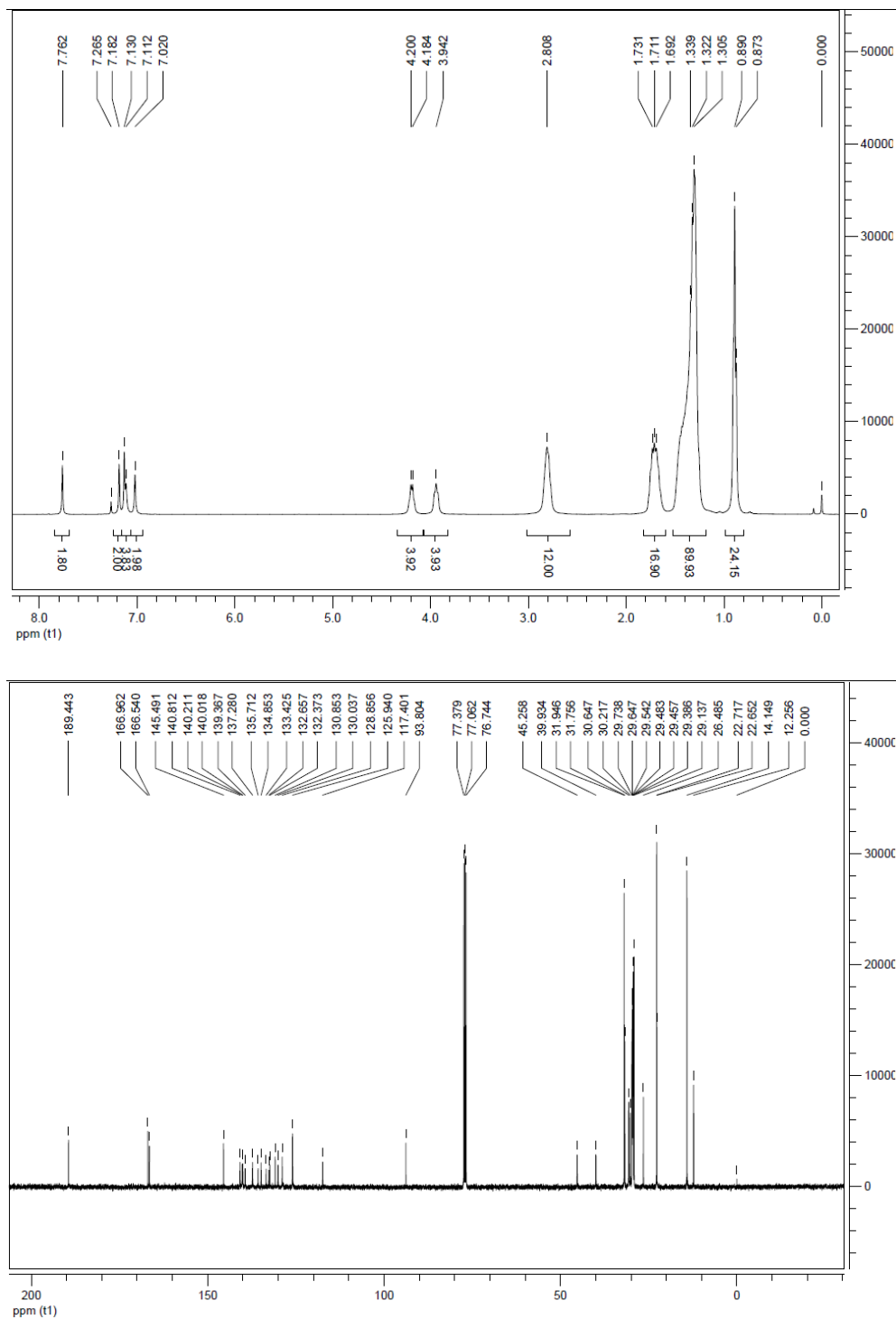


Figure S9. ^1H NMR (top) and ^{13}C NMR (below) spectrums of D2R(8+2)7T.

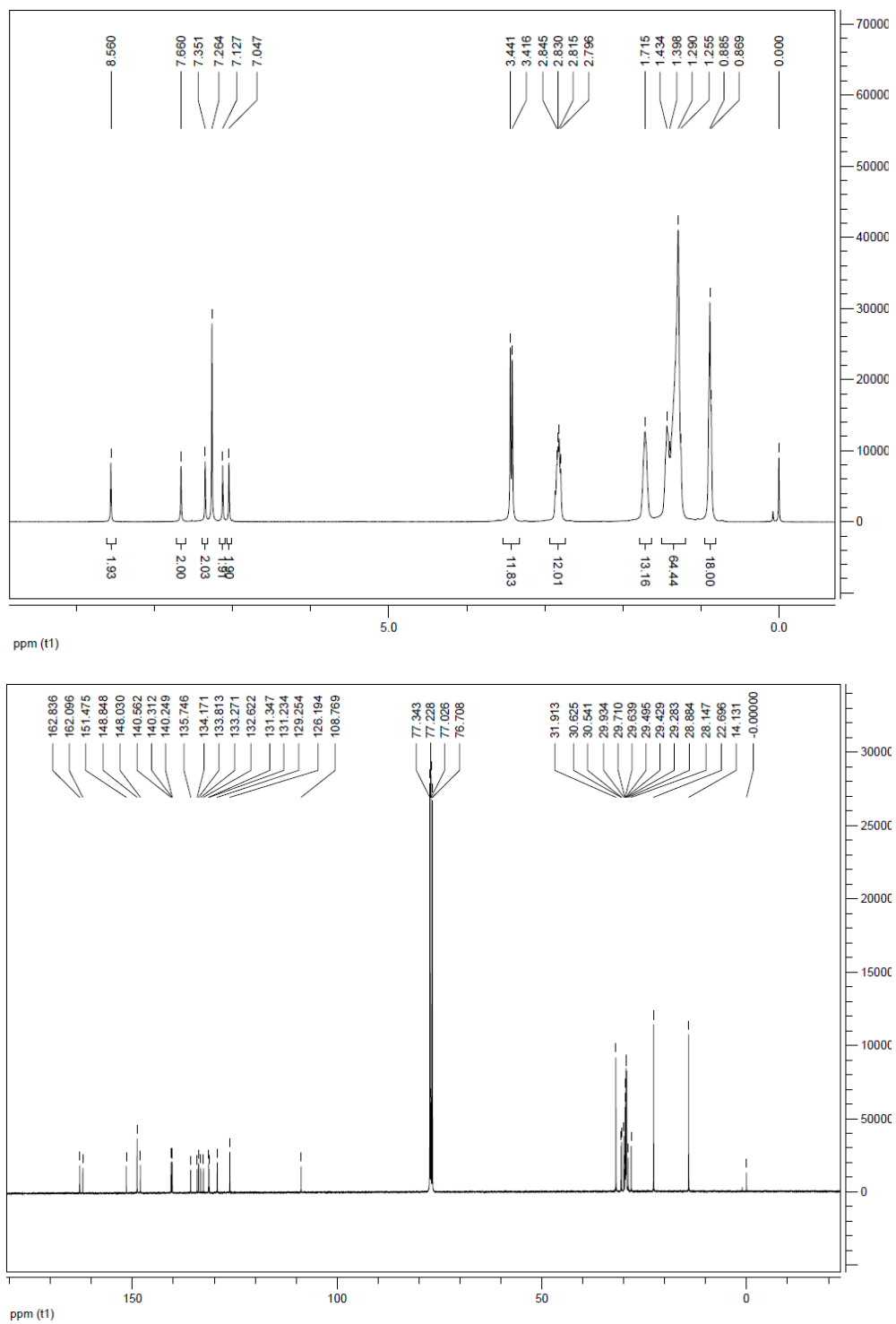


Figure S10. ^1H NMR (top) and ^{13}C NMR (below) spectra of DTDMP7T.

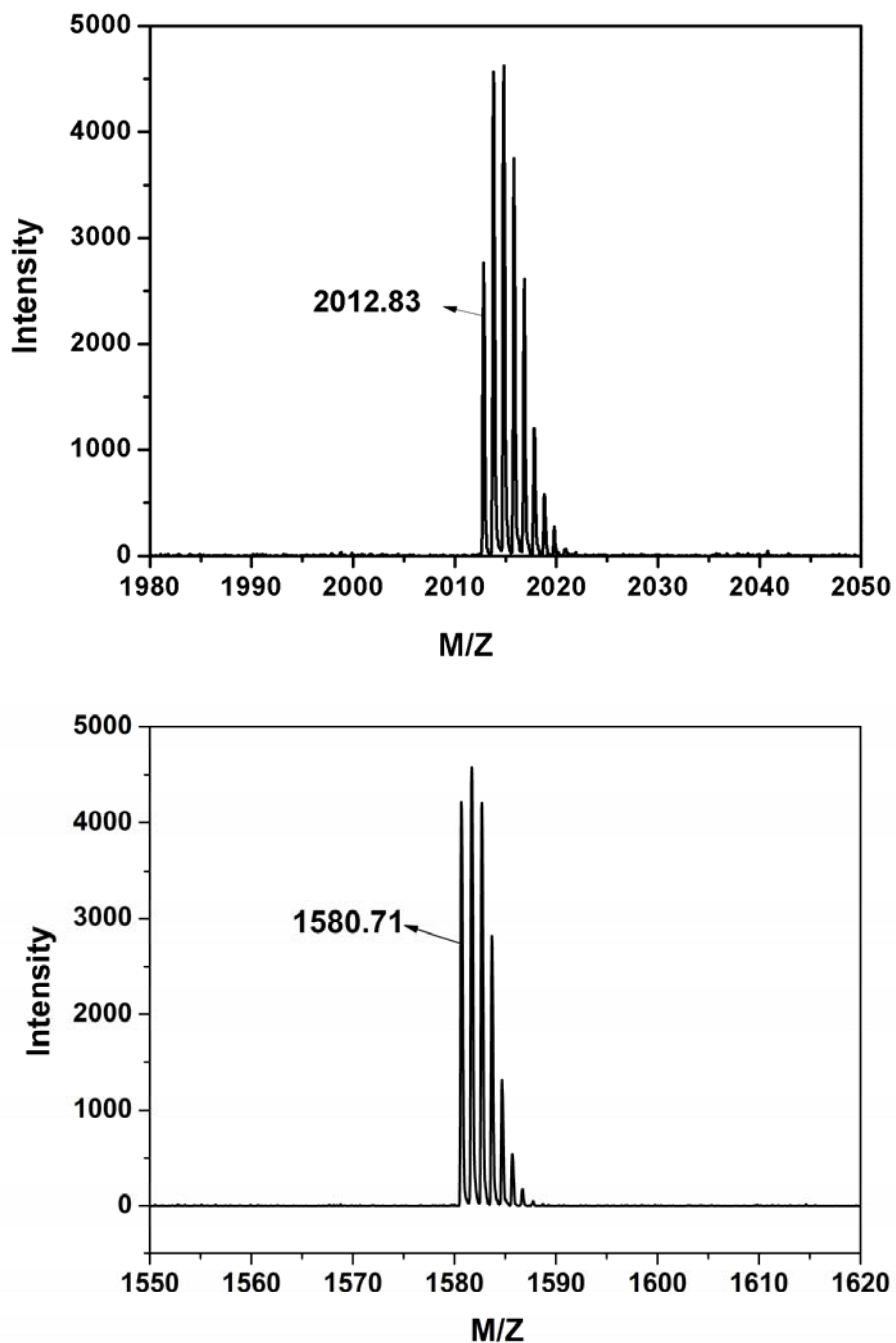


Figure S11. MS (MALDI-TOF) spectrums of D2R(8+2)7T (top) and DTDMP7T (below).

Section B configurations of our molecules

In order to investigate the exalty configuration of our molecules, we used ROSEY (rotating frame Overhauser effect spectroscopy) and the chemical shift in H NMR. At the same time, we

used density functional theory (DFT) with the Gaussian 09 model^[1] to investigate the most stable geometry. To our surprise, we find that the calculated geometry are in consistent with our experiment result for all the four molecules mentioned in our paper. The details are shown as follow.

(1) For DTDMP7T, we know that there are two possible conformations as shown in Figure 1B-a.

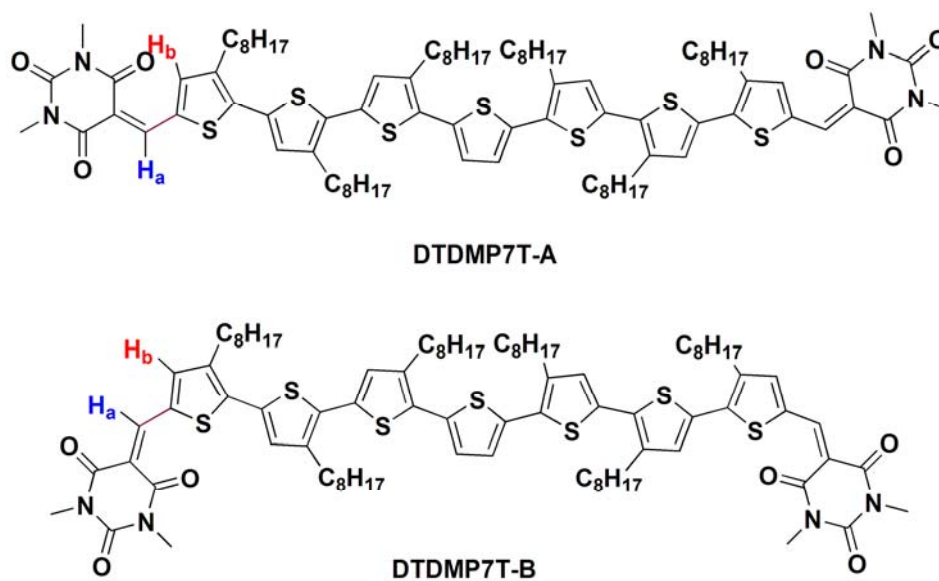


Figure 1B-a. Possible configurations of DTDMP7T

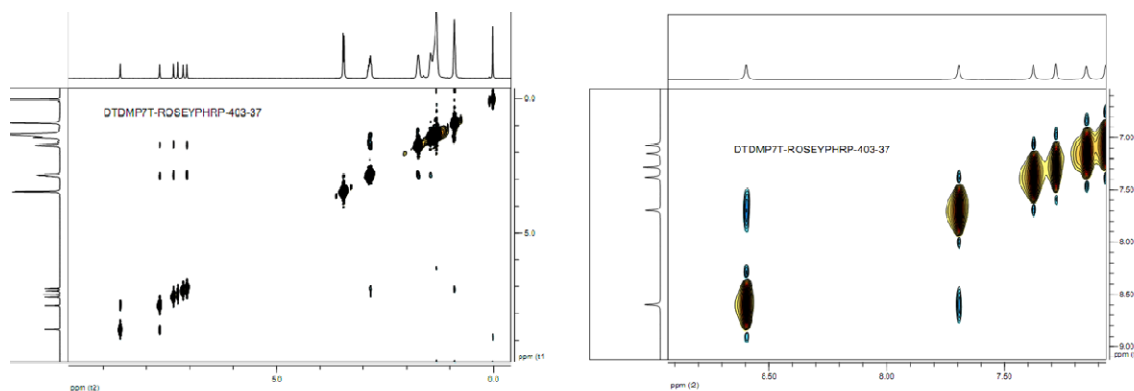


Figure 1B-b. Rosey of DTDMP7T (left is the full spectrum and right is the expand spectrum)

From the ROSEY spectrum, we can see that there is a distinct cross peak (H_a 8.57 to H_b 7.68),

which means that these two protons (H_a and H_b) are near in the space. So the result of our ROSEY experiment is that the configuration of DTDMP7T is DTDMP7T-B (Figure 1B-a).

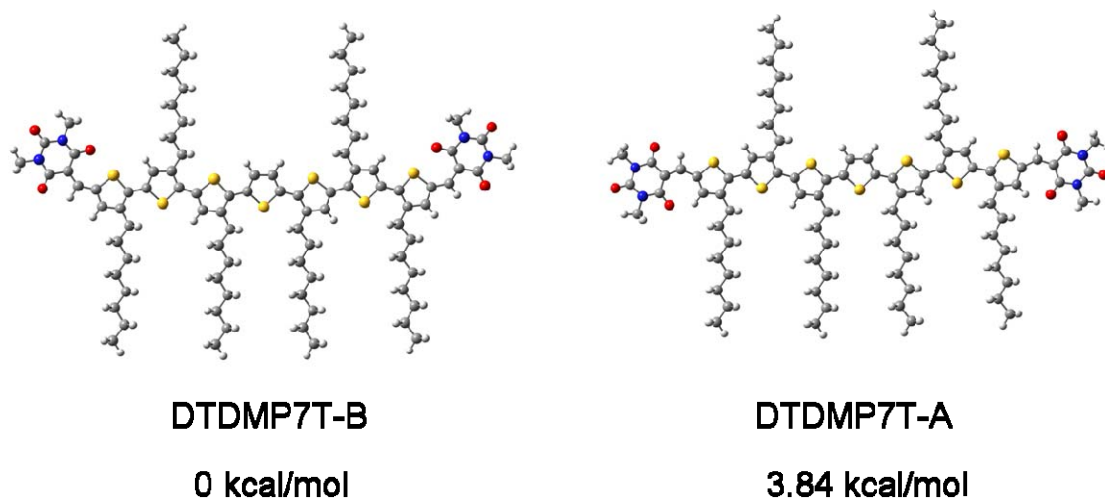


Figure 1B-c. Calculated result for DTDMP7T

In addition, the calculated result (Figure 1B-c) show that DTDMP7T-B is the most stable configuration between all these possible conformations of DTDMP7T. we concluded that if the single bond between the thiophene and acceptor (purple coloured) can rotate freely in the solution, DTDMP7T-B is the advantaged conformation. And , if the single bond between the thiophene and acceptor (purple coloured) can't rotate freely in the solution, DTDMP7T-B is the very configuration.

(2) For DCAO7T, the situation is more complex, for there are four possible conformations as shown in Figure 2B-a.

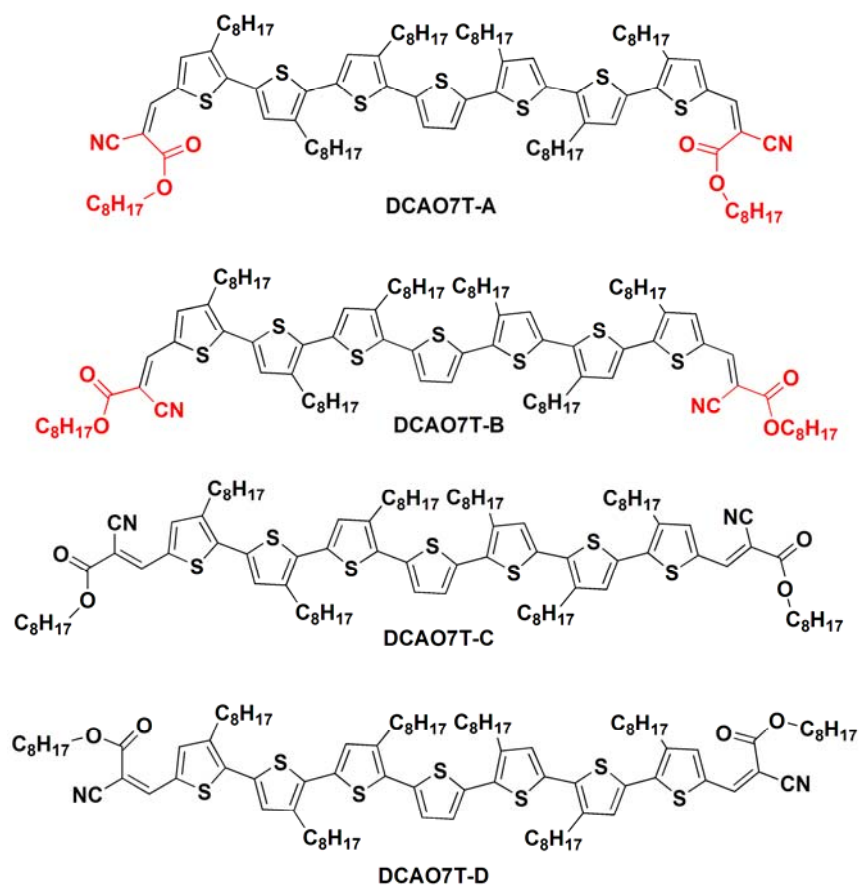


Figure 2B-a. Possible conformations of DTDMP7T

Rosey spectrum was carried out and shown in **Figure 2B-b**. From Rosey spectrum we can see that the DCAO7T-A and DCAO7T-B are the possible configurations as shown in Figure 2B-a. From references we know that the chemical shift of methine proton H_a as shown in Figure 2B-a are appeared at a lower field in the Z configuration than that of the E configuration. So, we show in the Figure 2B-c the chemical shift of some model molecules and the reaction condition.

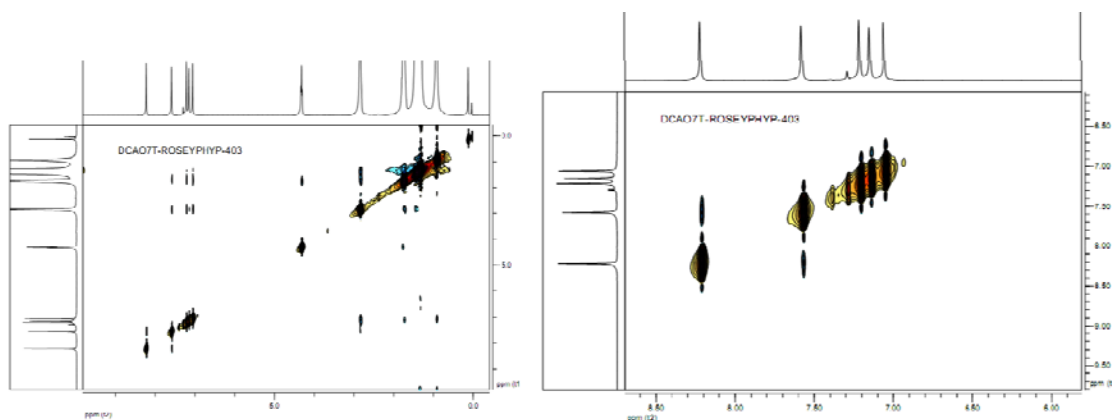
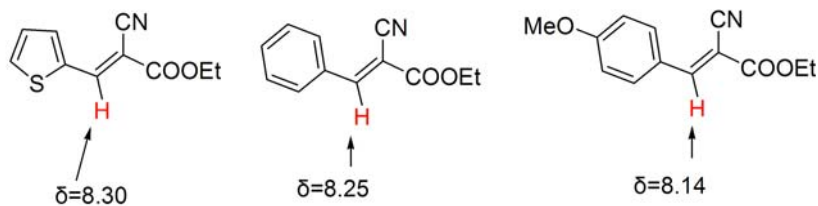
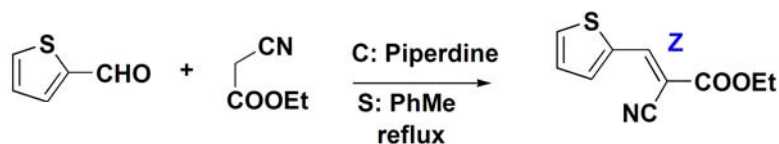


Figure 2B-b. Rosey of DCAO7T (left is the full spectrum and right is the expanded spectrum)



European Journal of Organic Chemistry,
(3), 546-551; 2004



European Jouran of Organic Chemistry,(1),137-142,2011

Figure 2B-c. Chemical shift of proton for some model compounds and the reaction condition.

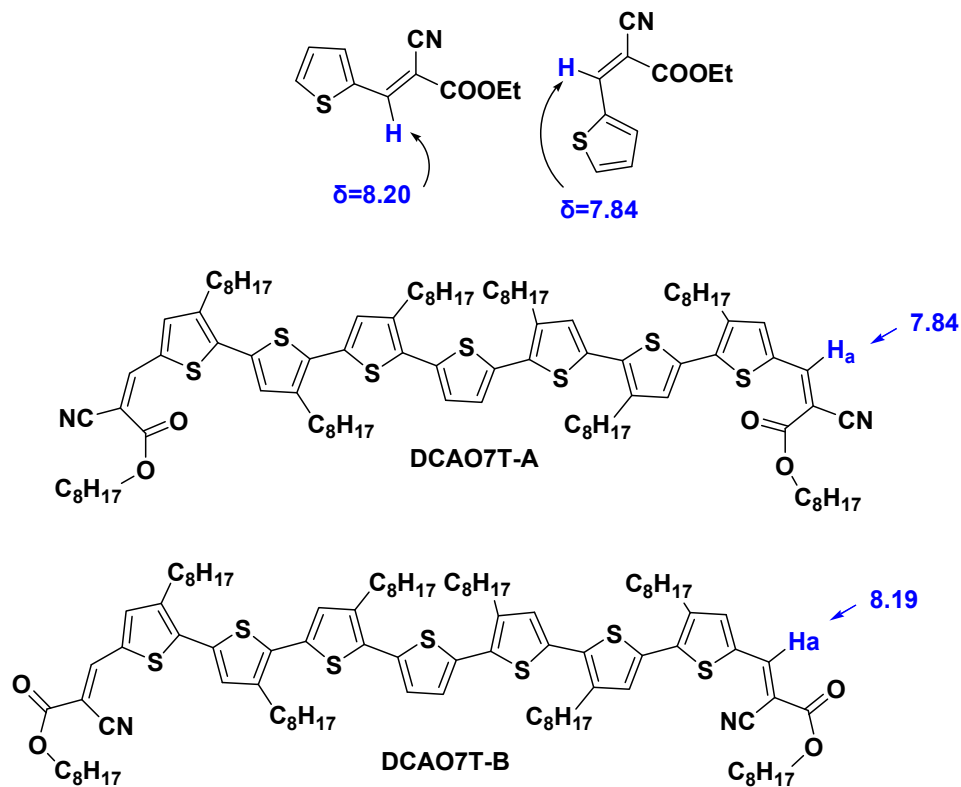


Figure 2B-d. Chemical shift of proton H_a for some model compounds and DCAO7T calculated by Chem. Office.

The Chemical shift of proton (H_a) by the H NMR for DCAO7T is 8.19 ppm (see Adv. Energy Mater. 2011, 1, 771–775). For the chemical shift of proton (H_a) and the reacton condition are similar to the model compounds (Figure 2B-c), we concluded that DCAO7T-B is the configuration of our molecule DCAO7T, which was also supported by the result predict by Chem. Office (Figure 2B-d).

In addition, the calculated result (Figure 2B-e) show that DCAO7T-B is the most stable configuration between all these possible configurations of DCAO7T (Figure 2B-e).

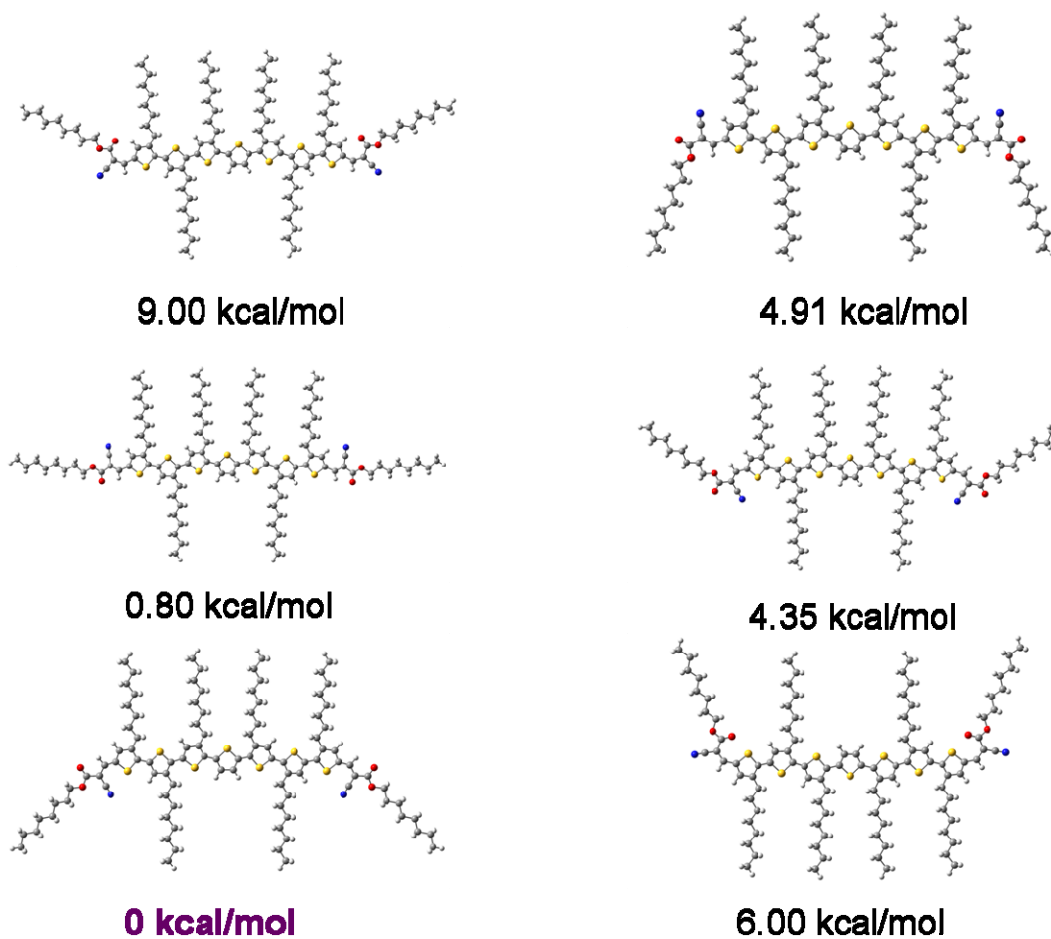


Figure 2B-e Calculated result for DCAO7T

For all above, we conclude that DCAO7T-B is the exact configuration for DCAO7T.

(3) For DERHD7T, the situation is similar to that of DCAO7T. There are four possible configurations as shown in Figure 3B-a.

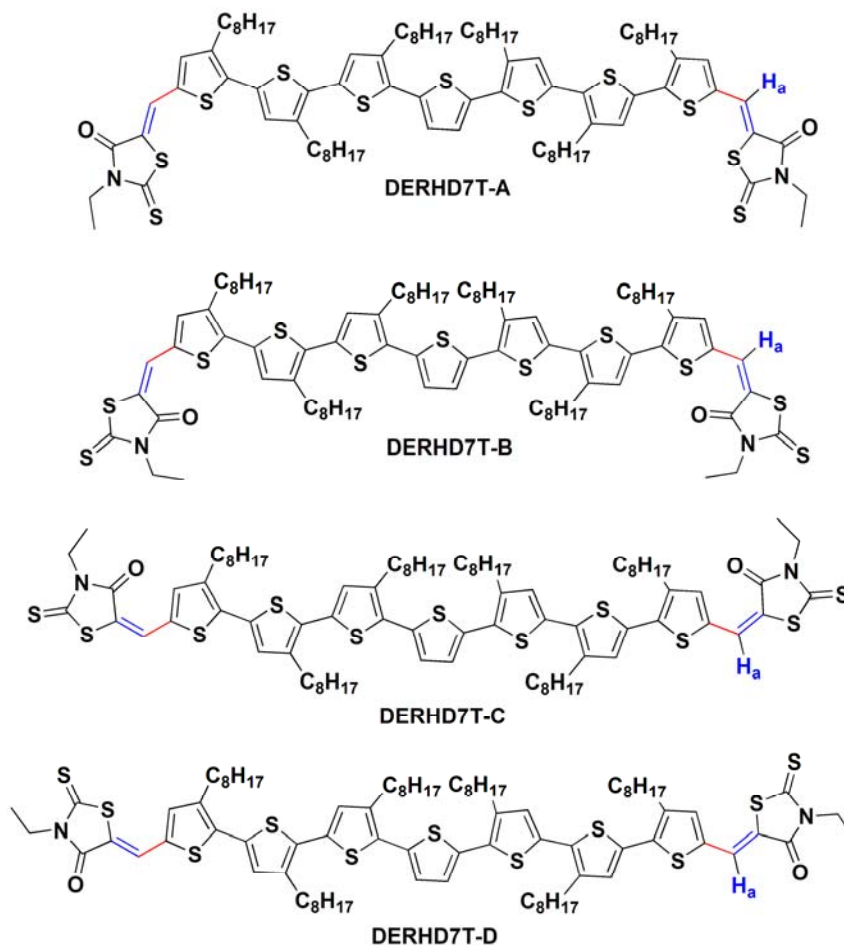
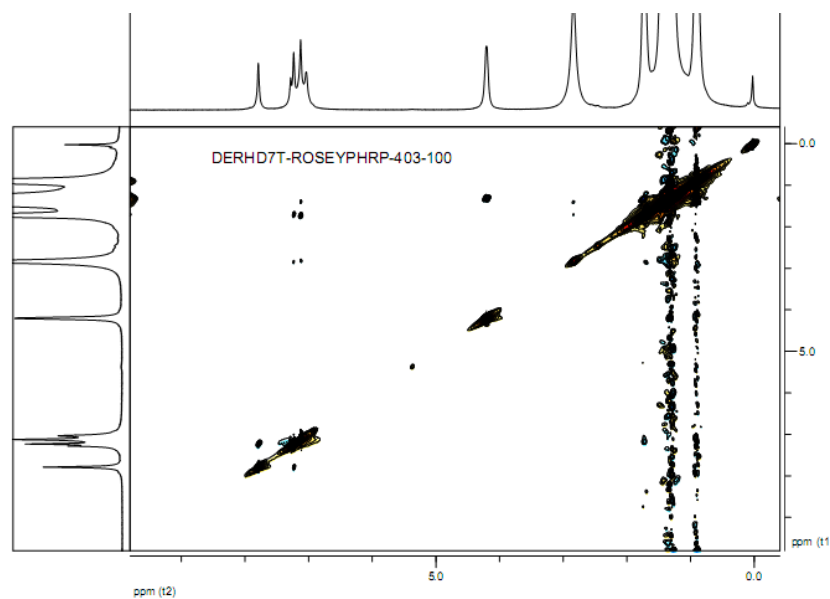


Figure 3B-a. Possible configurations of DERHD7T



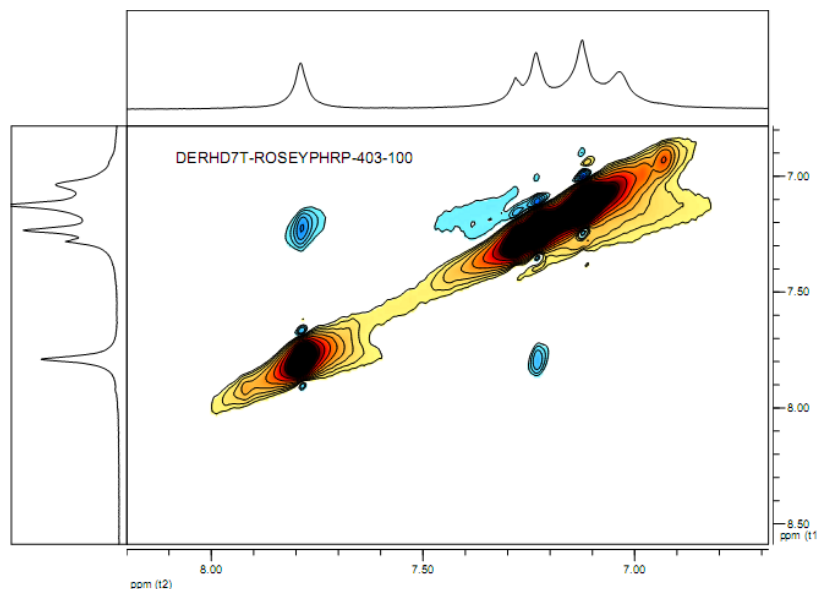


Figure 3B-b. ROSEY of DERHD7T (top is the full spectrum and below is the expanded spectrum)

From ROSEY spectrum (Figure 3B-b) we can see that the DERHD7T-A and DERHD7T-B are the possible configurations as shown in Figure 3B-a. From references we know that the chemical shift of methine proton H_a as shown in Figure 3B-a are appeared at a lower field in the Z configuration than that of the E configuration (*Chem. Pharm. Bull.* 39(6) 1440-1145 (1991)). So, we show in the Figure 3B-c the chemical shift of methine proton for some model molecules and the reaction condition.

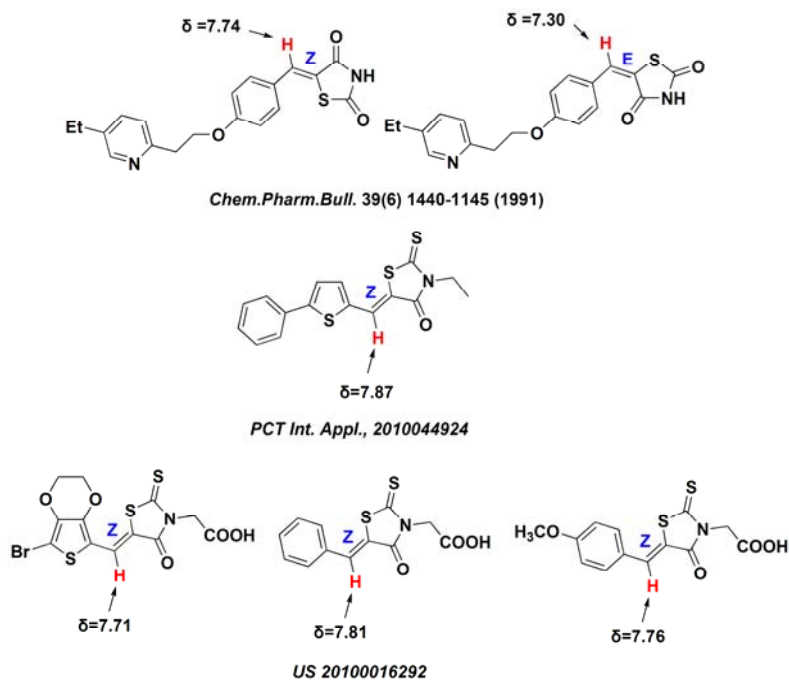


Figure 3B-c. Chemical shift of proton for some model compounds

The Chemical shift of proton (H_a) by the 1H NMR for our DERHD7T is 7.76 ppm. Compared with the model compounds in reference (Figure 3B-c), we concluded that DERHD7T-A is the very

configuration of our molecule DERHD7T.

In addition, the calculated result (Figure 3B-d) show that DERHD7T-A is the most stable configuration between all these possible conformations of DERHD7T.

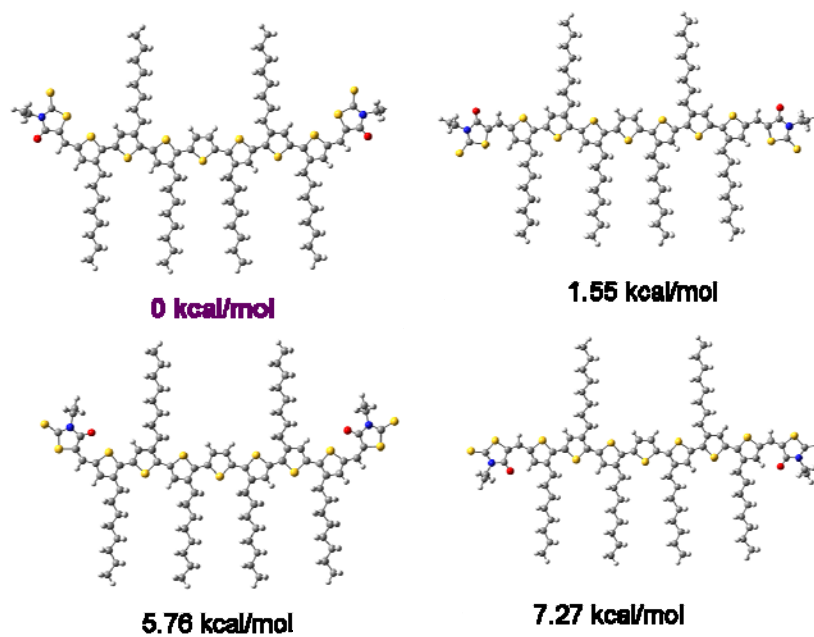


Figure 3B-d . Calculated result for DERHD7T

For all above, we conclude that DERHD7T-A is the exact configuration for DERHD7T.

(4) For [D2R\(8+2\)7T](#), the situation is similar to that of DERHD7T. There are four possible configurations as shown in Figure 4B-a.

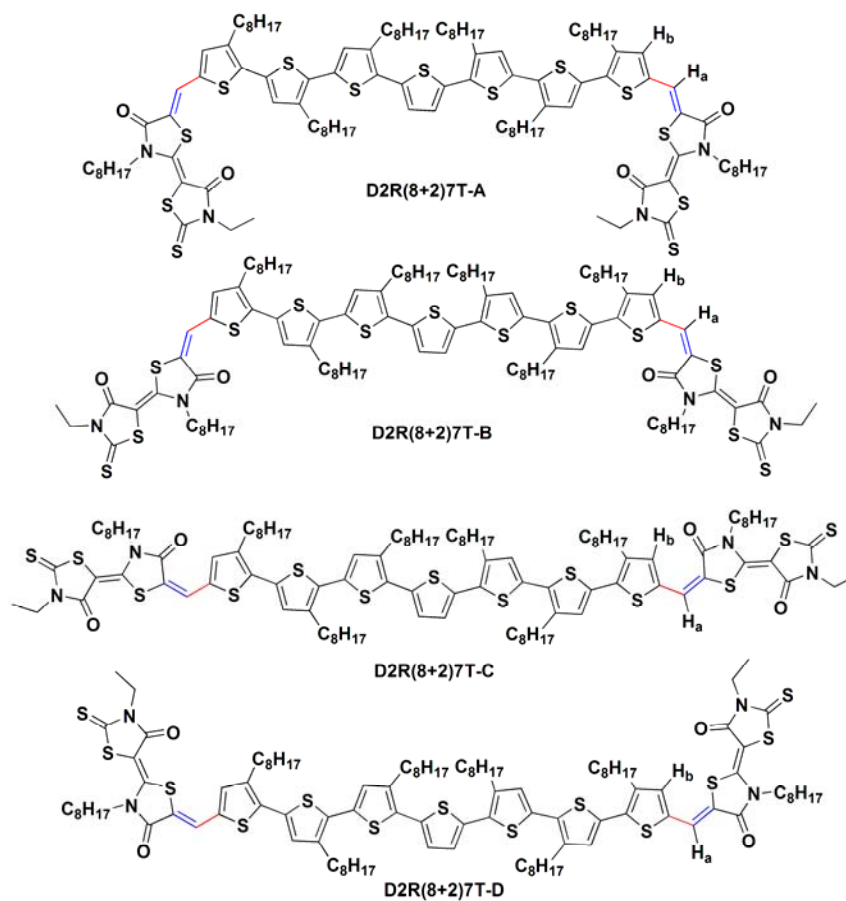


Figure 4B-a. Possible configurations of D2R(8+2)7T

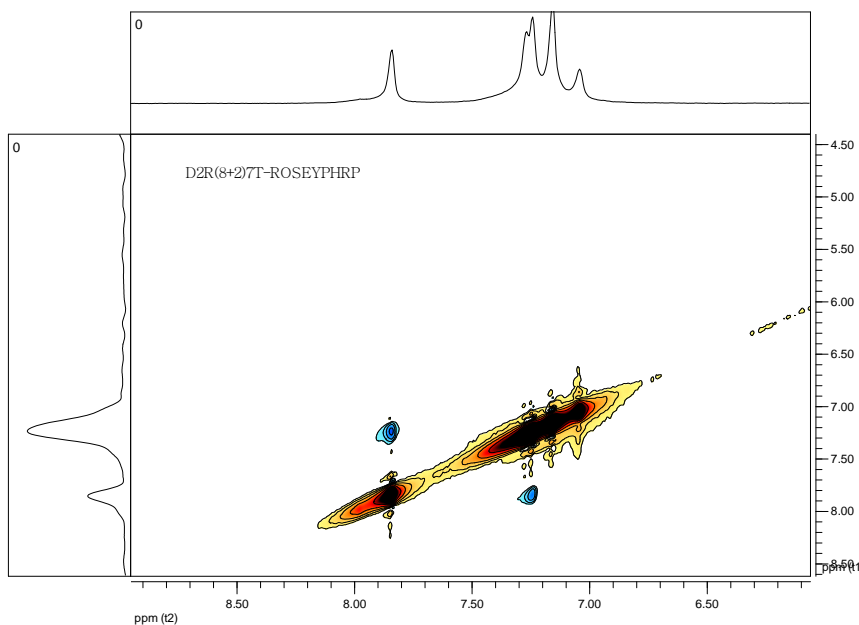
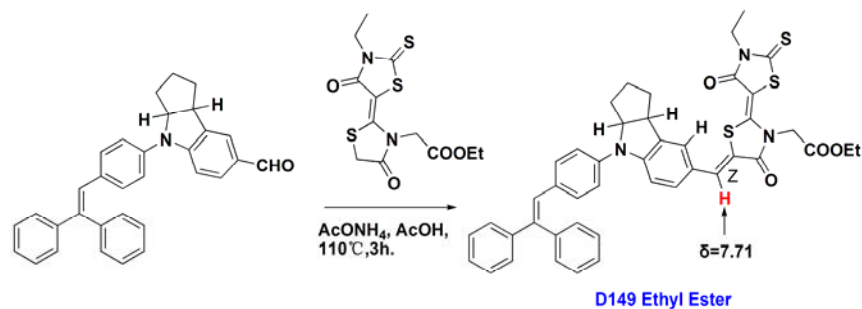


Figure 4B-b. Rosette of D2R(8+2)7T (top is the full spectrum and below is the expanded spectrum)

From Rosette spectrum (Figure 4B-b) we can see that the D2R(8+2)7T-A and D2R(8+2)7T-B are the possible configurations as shown in Figure 4B-a. From references we know that the chemical shift of methine proton H_a as shown in Figure 4B-a are appeared at a lower field in the Z

configuration than that of the E configuration (*Chem. Pharm. Bull.* 39(6) 1440-1145 (1991)). So, we show in the Figure 4B-c the chemical shift model molecule **D149 Ethyl Ester** and the reaction condition.



Bulletin of the Chemical Society of Japan (2010), 83(6), 709-711.

Figure 4B-c. Chemical shift of methine proton for **D149 Ethyl Ester** and reaction condition.

The Chemical shift of proton (H_a) by the 1H NMR for our **D2R(8+2)7T** is 7.78 ppm, similar to that of **D149 Ethyl Ester**. What's more, the reaction condition of **D2R(8+2)7T-A** is the same as that of **D149 Ethyl Ester**, thus we concluded that **D2R(8+2)7T-A** is the very configuration of our molecule **D2R(8+2)7T**.

In addition, the calculated result (Figure 4B-d) shown that **D2R(8+2)7T-A** is the most stable configuration between all the possible configuration of **D2R(8+2)7T**.

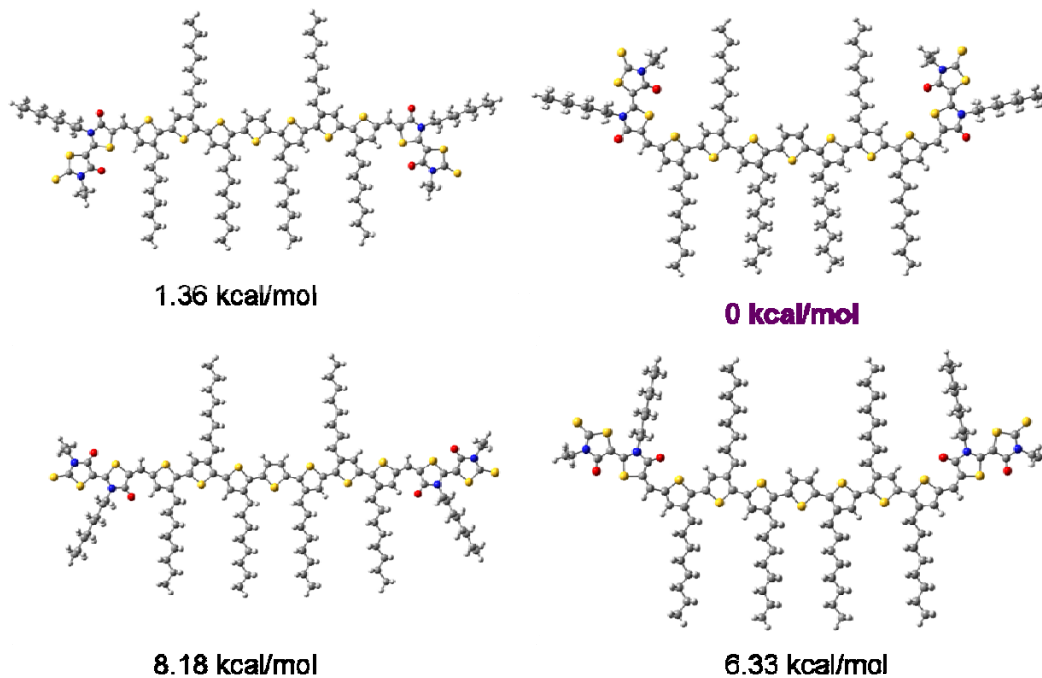


Figure 4B-d. Calculated result for **D2R(8+2)7T**

In summary, the configurations of our four molecules are shown as Figure B.

1. For **DCAO7T**, **DERHD7T** and **D2R(8+2)7T**, the methine moiety between the thiophene

and acceptor unit are all Z-form.

2. The hydrogen atom at the methine moiety (H_a) and hydrogen atom attached to the side thiophene (H_b) is cis-form.
3. The configurations of our molecules are the most thermodynamically stable configurations.

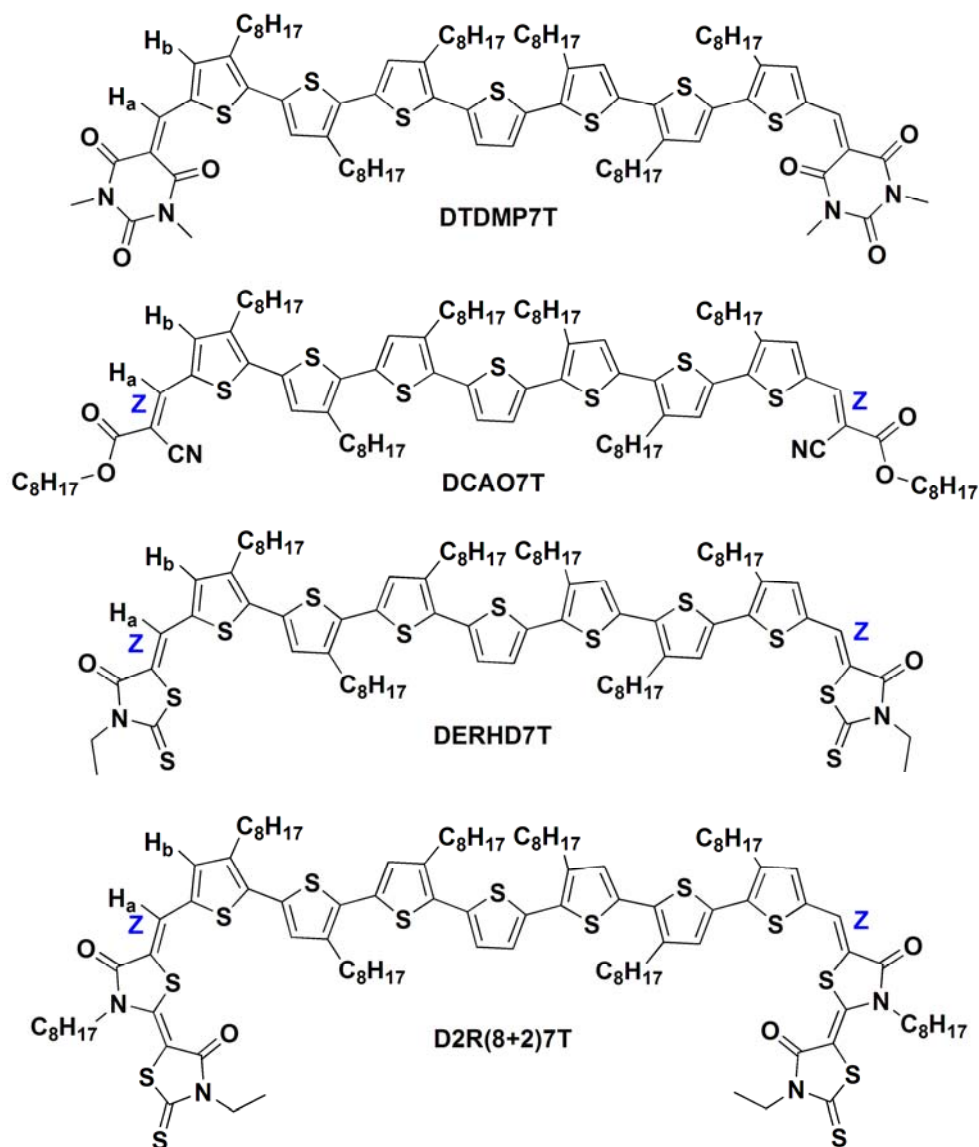


Figure B. configuration of DTDMP7T, DCAO7T, DERHD7T and D2R(8+2)7T

Reference:

-
- [1] Gaussian 09, Revision B.01,
M. J. Frisch, G. W. Trucks, H. B. Schlegel, G. E. Scuseria, M. A. Robb, J. R. Cheeseman, G.

Scalmani, V. Barone, B. Mennucci, G. A. Petersson, H. Nakatsuji, M. Caricato, X. Li, H. P. Hratchian, A. F. Izmaylov, J. Bloino, G. Zheng, J. L. Sonnenberg, M. Hada, M. Ehara, K. Toyota, R. Fukuda, J. Hasegawa, M. Ishida, T. Nakajima, Y. Honda, O. Kitao, H. Nakai, T. Vreven, J. A. Montgomery, Jr., J. E. Peralta, F. Ogliaro, M. Bearpark, J. J. Heyd, E. Brothers, K. N. Kudin, V. N. Staroverov, T. Keith, R. Kobayashi, J. Normand, K. Raghavachari, A. Rendell, J. C. Burant, S. S. Iyengar, J. Tomasi, M. Cossi, N. Rega, J. M. Millam, M. Klene, J. E. Knox, J. B. Cross, V. Bakken, C. Adamo, J. Jaramillo, R. Gomperts, R. E. Stratmann, O. Yazyev, A. J. Austin, R. Cammi, C. Pomelli, J. W. Ochterski, R. L. Martin, K. Morokuma, V. G. Zakrzewski, G. A. Voth, P. Salvador, J. J. Dannenberg, S. Dapprich, A. D. Daniels, O. Farkas, J. B. Foresman, J. V. Ortiz, J. Cioslowski, and D. J. Fox, Gaussian, Inc., Wallingford CT, 2010.